Microporous and Mesoporous Materials 184 (2014) 21–27

Contents lists available at ScienceDirect

Microporous and Mesoporous Materials

journal homepage: www.elsevier.com/locate/micromeso

Review

Experiments and simulations on separating a CO_2/CH_4 mixture using K-KFI at low and high pressures

Jiangfeng Yang [a], Rajamani Krishna [b], Junmin Li [a], Jinping Li [a,*]

[a] Research Institute of Special Chemicals, Taiyuan University of Technology, Taiyuan 030024, Shanxi, PR China
[b] Van 't Hoff Institute for Molecular Sciences, University of Amsterdam, Science Park 904, 1098 XH Amsterdam, The Netherlands

ARTICLE INFO

Article history:
Received 13 August 2013
Received in revised form 17 September 2013
Accepted 18 September 2013
Available online 27 September 2013

Keywords:
Separate CO_2/CH_4
Zeolite
K-KFI
Simulation

ABSTRACT

Separation of CO_2 from CH_4 is needed in order to use low-quality biogas or landfill gas and to reduce greenhouse gas emissions. To study the separation of a CO_2/CH_4 gas mixture, K-KFI (Si/Al = 4.59) sorbent was synthesized and pelletized. We performed breakthrough experiments at flow rates of 16.6 and 30 N mL/min under ambient temperature and pressure (298 K, 100 kPa). The breakthrough experiments results showed that K-KFI separated a 40%/60% mixture of CO_2/CH_4 better than a 50%/50% mixture. Furthermore, the separation performance of K-KFI is superior to that of commercial sorbents zeolite-5A and 13X under the same conditions. Simulations of the breakthrough of binary mixed gases CO_2/CH_4 = 40%/60%, yield results that are in good agreement with our experimental data. By performing breakthrough simulations at a total pressure of 2 MPa, we demonstrated that pure CH_4 can be separated from CO_2/CH_4 gas mixtures under high pressure, and that pure CH_4 can be recovered in the initial stages of the breakthrough.

Contents

1. Introduction

Compared with fossil fuels such as petroleum and coal, natural gas produces less CO_2 per energy unit; thus, it is regarded as a cleaner energy source. Biogas and landfill gas are supplemental gas energy sources, which mainly contain CH_4. As an effective complement to conventional natural gas, actively developing and using biogas and landfill gas has tangible benefits. However, CO_2 impurities in these gases (30–50% in biogas and landfill gas) could reduce their heating value and cause equipment and pipeline corrosion [1]. Pipeline specifications generally require that the proportion of CO_2 in the

* Corresponding author. Tel./fax: +86 351 6010908.
E-mail address: jpli211@hotmail.com (J. Li).

1387-1811/$ - see front matter © 2013 Elsevier Inc. All rights reserved.
http://dx.doi.org/10.1016/j.micromeso.2013.09.026

natural gas used be lower than 2%; thus, the CO_2 content of the unconventional gas used must be reduced before pipeline transport [2]. Additionally, CO_2 and CH_4 are greenhouse gases, which contribute significantly to global warming. About 60% of the global warming effect is caused by CO_2 [3], while CH_4 much more strongly influences global warming per unit volume than does CO_2 [4]. Thus, separating CO_2 from CH_4 is needed in order to use low-quality unconventional gas while reducing greenhouse gas emissions [5].

Various technologies have been developed to separate CO_2/CH_4 mixtures; these techniques include absorption, membrane separation, and adsorption. Among these, adsorption has received intense interest because of its great advantages, such as high energy efficiency, ease of control, and low capital investment costs [6]. The main adsorbents evaluated for adsorptive separation of CO_2/CH_4 binary mixtures include zeolites [7–9], metal–organic frameworks (MOFs) [10–12], silicas [13,14], and carbon-based materials [15–18]. Zeolites, such as zeolite 5A and 13X, are the most industrially and commercially used adsorbents for CO_2/CH_4 separation [19,20]. These zeolites are stable at high temperatures and pressures, have low heat capacity and high selectivity of CO_2, are homogeneous, and allow for easy replacement of extra-framework cations [21]. The properties of these aluminosilicate minerals have led to their use in a myriad of industrial applications in catalysis and separation.

In recent years, researchers have studied a variety of zeolites structures with small pore sizes and 8-membered rings, such as CHA, LEV, and KFI for gas-adsorption separation [7,22–24]; these studies showed that these structures have higher selectivity of CO_2 from CH_4 than do the traditional zeolites LTA and FAU [25]. Unlike LTA and FAU, synthesizing CHA and KFI is environmentally friendly because they do not need an organic template agent when being prepared. The surface area and pore size of KFI are slightly larger than those of CHA; thus, gases diffuse more quickly through its pores. Because of this property, most researchers focus on CO_2, CH_4, N_2, and H_2O adsorption using KFI with different balance ions.

Remy et al. studied the adsorption and separation of CO_2 using ZK-5 (Framework Type Code: KFI) zeolites with different types of cations and Si/Al ratios. Their results showed that Li-ZK-5 and Na-ZK-5 had the highest capacities and high selectivities, similar to the benchmark: zeolite 13X [23]. Lobo's research group focused on synthesizing the zeolite ZK-5 exchanged with different cations (H^+, Li^+, Na^+, K^+, Mg^{2+}, Ca^{2+}) and its use as a CO_2 adsorbent. The results of this CO_2 adsorption analysis showed that Mg-ZK-5 was the most promising adsorbent for pressure swing adsorption (PSA) applications because it had the highest working capacity ($\Delta N_{CO_2} = 0.25\ mmol\ g^{-1}$) of the adsorbents studied, excellent selectivity ($a_{CO_2/N_2} = 121$), and low isosteric heat. Li-, Na-, and K-ZK-5 also had good working capacity and excellent selectivity; thus, they are promising CO_2 adsorbents for the vacuum swing adsorption (VSA) working region [22].

The KFI starting material always contains K^+, called K-ZK-5 or K-KFI. According to published data on CO_2 adsorption using K-KFI, we found that higher Si/Al content led to its higher capacity, caused by the higher surface area of the structure with less K^+ (Table 1). Thus, in this work KFI was synthesized with a higher Si/Al content of 4.59. Justified by recent studies, we also studied CO_2 adsorption using KFI with different cations [7]. Few reports have collected and analyzed breakthrough data on separating CO_2/CH_4 binary mixtures using KFI, especially for different gas mixture ratios and pressures. Thus, CO_2/CH_4 binary mixture gas breakthrough at two ratios: 50%/50 % and 40%/60 %, and compared these data with those of commercial zeolite-5A and 13X. Additionally, we simulated CO_2/CH_4 separation up to a high pressure of 2 MPa using breakthrough simulations.

Table 1
CO_2 adsorption capacity on K-KFI with different Si/Al.

Material	CO_2 (mmol/g)	Temperature (K)	Si/Al	References
LS-K-KFI	3	303	1.67	[22]
K-ZK-5	3.4	303	3.67	[22]
K-ZK-5	3.9	303	4.70	[23]

2. Experimental

2.1. Materials and methods

KFI was synthesized using a reported procedure using K^+ as the balance cation; this material is known as K-KFI [7], and more detailed about synthesis conditions are provided in the Supplementary material. Zeolite-5A (Si/Al = 1, Aladdin, China) and zeolite-13X (Si/Al = 1.2, Aladdin, China) were used without further purification. To pelletize the zeolites, the zeolite powder was formed into tablets at 10 MPa and then crushed into granules, after which uniform particles were filtered out.

2.2. Characterization and gas adsorption measurements

The crystallinity and phase purity of the zeolites were measured using powder X-ray diffraction (XRD) using a Rigaku Mini Flex II X-ray diffractometer with Cu Kα radiation at 30 kV and 15 mA. The 2θ scanning range was 5–40° at a rate of 1°/min. Morphological data were acquired by scanning electron microscopy (SEM) using a Rigaku TM-3000 operated at 15.0 kV. Samples were coated with gold before performed microscopy in order to increase their conductivity.

The purity of the methane used was 99.95%, and that of the carbon dioxide used was 99.99%. Adsorption isotherms at high pressure were measured on an intelligent gravimetric analyzer (IGA 001, Hiden, UK). Prior to measuring an isotherm, a 50 mg sample was pre-dried at a reduced pressure and then outgassed overnight at 400 °C under a high vacuum until no further weight loss was observed. Each adsorption/desorption step was allowed to approach equilibrium over a period of 20–30 min, and all the isotherms for each gas were measured from a single sample.

2.3. Breakthrough experiments

A schematic of the experimental setup for the breakthrough experiments is shown in Fig. 1. Block samples were prepared, which were collected using 40–80 mesh and then loaded into the adsorption column ($\Phi 10 \times 150$ mm). First, allowed for in situ activation of the adsorbent under pure (99.999%) He flow, after which we allowed the raw mixed gas (CO_2 and CH_4) to flow and collected the outlet gas emissions over intervals of 0.5–1.5 min. Analyzed the outgas composition and concentration using gas chromatography (Shimadzu 2014C, separation column was loaded with 13X; for balance calculations and the gas-content analysis process, see Supplement Information). All separation experiments were performed at 298 K with a total flow rate ranging from 16.6 to 30.0 N mL/min. Over the course of each breakthrough test, no more He was needed.

3. Results and discussion

3.1. Synthesis and characterization

Synthesis of functional molecular sieve without template agent is considered to be environment-friendly production method; it has been always a hot topic research [26,27]. K-KFI was synthesized without organic templating agent [28,29] and used in this work, the data of synthesis and character of K-KFI has been

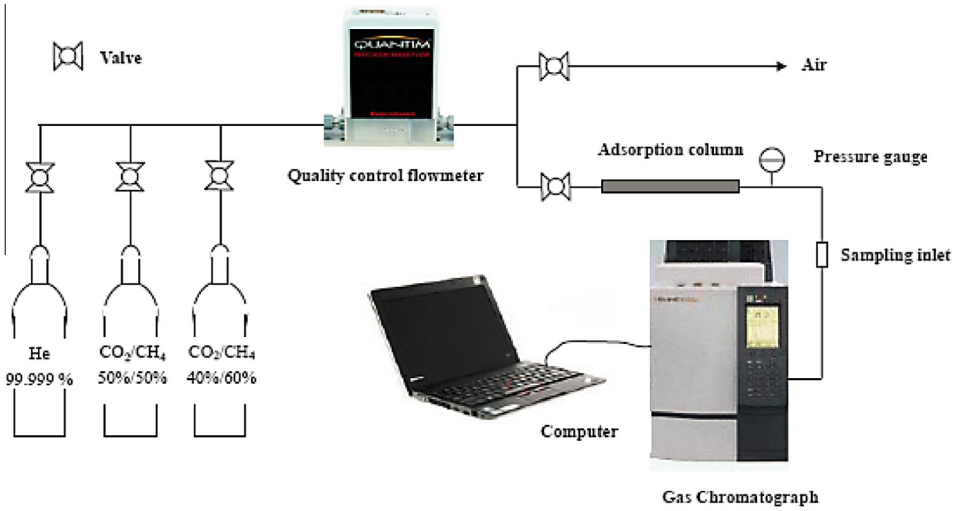

Fig. 1. The equipment of CO_2/CH_4 Separation test system.

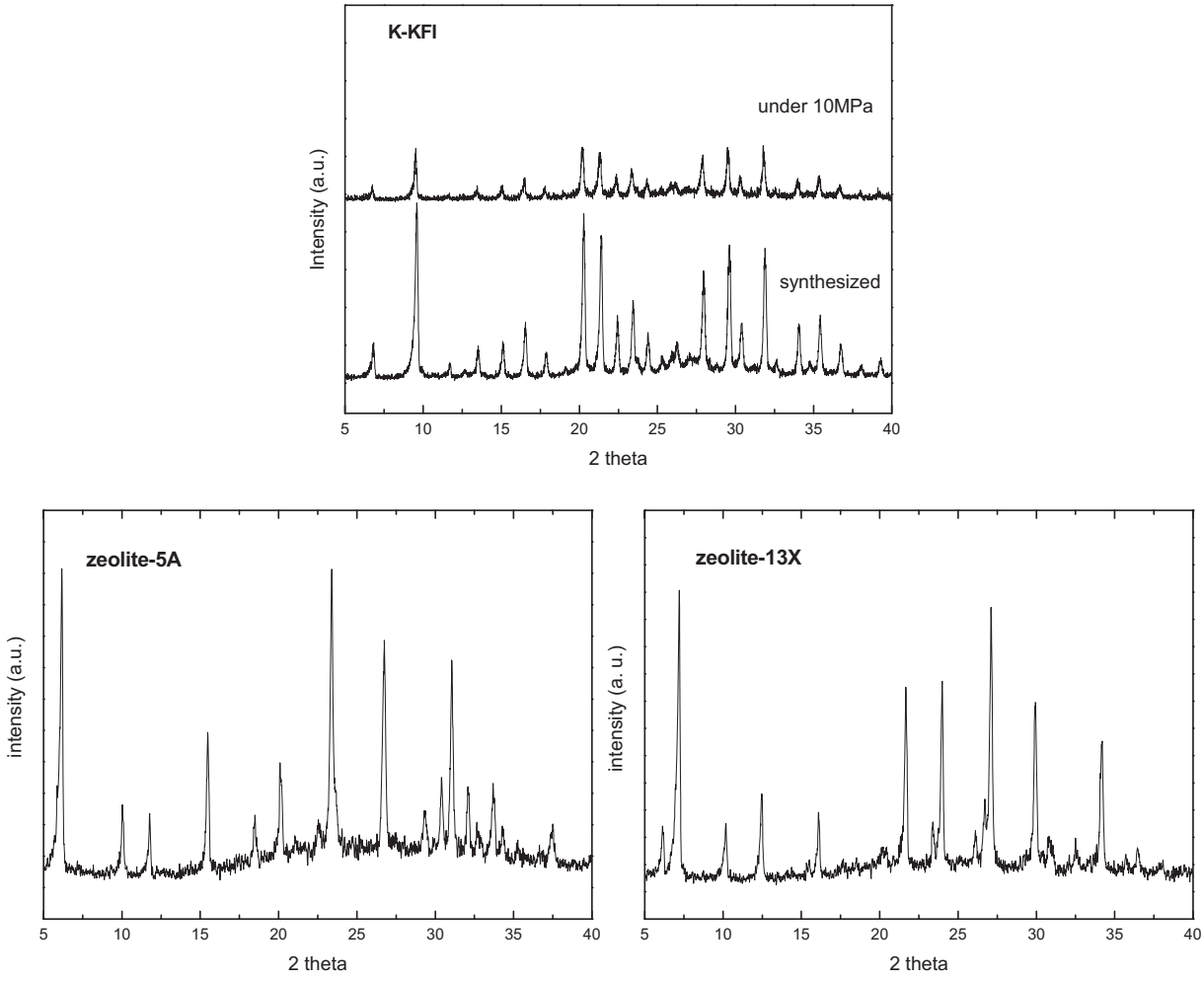

Fig. 2. XRD patterns of K-KFI, zeolite-5A and 13X.

published [7]. The Supplementary material provides more details about raw materials and synthesis conditions.

To avoid large pressure drops during gas-phase separation, the packed bed should not be filled with powder. Instead, aggregates – such as pellets – of adsorbent crystals with sufficiently high pressure stability must be prepared. Thus, Blocks of the K-KFI powder be prepared at a high pressure of 10 MPa and then crushed the blocks into granules; these granules were used in the separation column. XRD patterns show that the peak positions and relative diffraction intensity of block K-KFI was similar to those of the

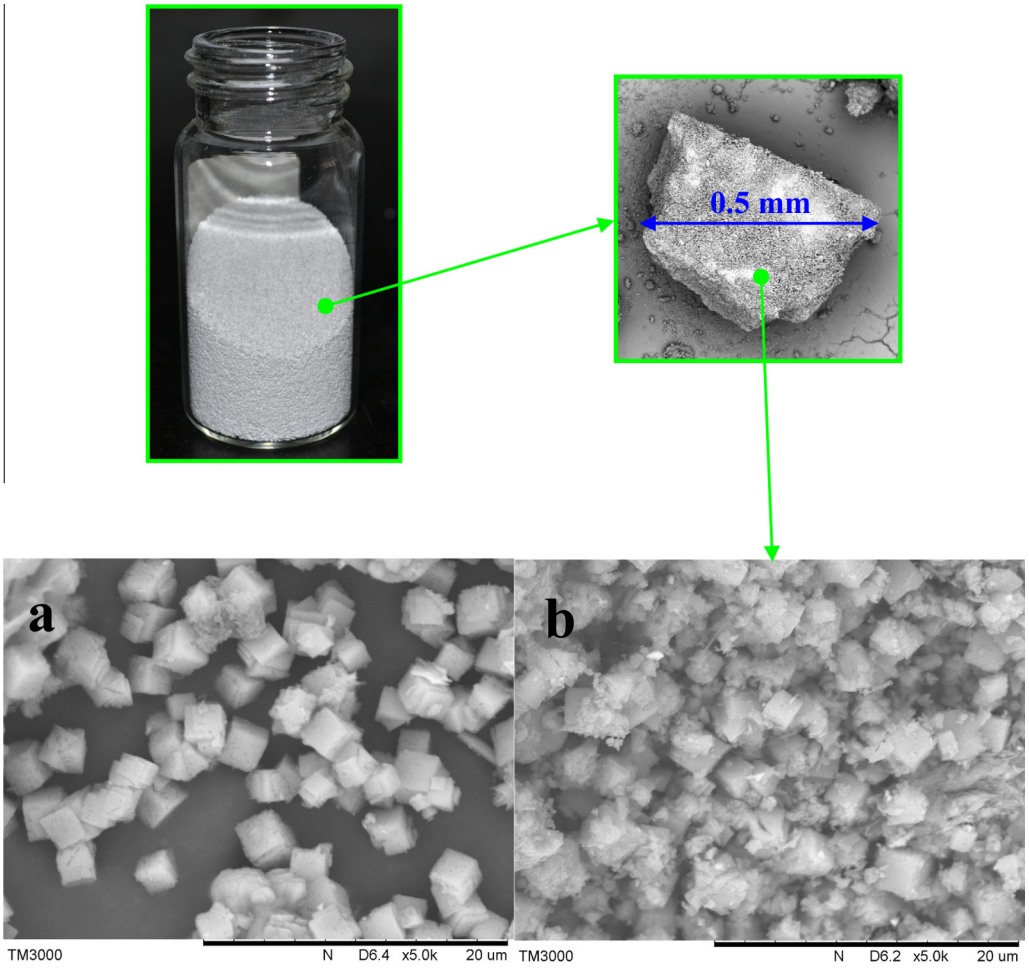

Fig. 3. The SEM of K-KFI. (a) Synthesized powder; (b) pelletized).

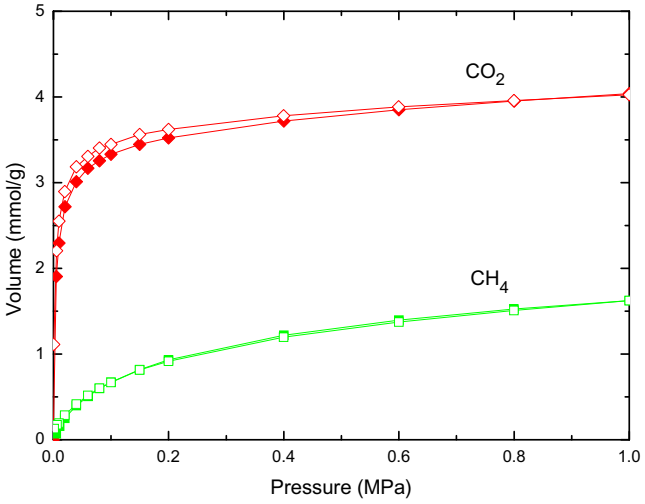

Fig. 4. Adsorption CO_2 and CH_4 on K-KFI under 1 Mpa.

powder sample; thus, it can be inferred that the structure of K-KFI was not changed at the high pressure used (Fig. 2). By comparing with standard XRD patterns of zeolite structures from a database, we determined that the zeolite-5A and 13X materials used had standard structures.

Fig. 3 shows photographs and SEM images of the pellets; the size of the K-KFI pellets is about 0.5 mm. The distance between crystals in the pelletized K-KFI sample was much smaller than in the powder sample, and its crystal morphology was denser. The micro surface area of the pelletized K-KFI sample was lower than that of the powder sample because its outer surface area was reduced. However, this difference did not affect the separation test, where the inner surface and porosity played key roles.

3.2. Breakthrough test

Fig. 4 shows that the adsorption capacity of CO_2 and CH_4 of the pelletized sample was very stable compared with the powder sample [7]. Therefore, the separation test will not be affected by different adsorbent particle size. When flowing 50%/50% CO_2/CH_4 through the adsorption bed, the CH_4 breakthrough time was 1.82 min when the mixture-gas flow rate was 16.6 N mL/min (STP) (Fig. 5a). Helium was driven out quickly, and the CH_4 concentration quickly reached its peak in less than 0.5 min. The breakthrough time of CO_2 was 9.43 min; thus the difference in breakthrough time for CO_2 and CH_4 was 7.61 min (a longer time difference leads to better separation). Upon accelerating the mixture-gas flow rate to 30 N mL/min (45% higher than 16.6 N mL/min), the breakthrough time of CH_4 decreased to less than 1 min, 46% shorter than that at 16.6 N mL/min (Fig. 5b). For the faster flow rate, the breakthrough time of CO_2 decreased to 5.30 min, 45 % shorter than the slower flow rate; thus, the difference in CO_2 and CH_4 breakthrough times was 4.32 min for the faster flow rate. The average time decreased by 44 %, equal to the percentage increase in the mixture-gas flow rate. This result indicates that the

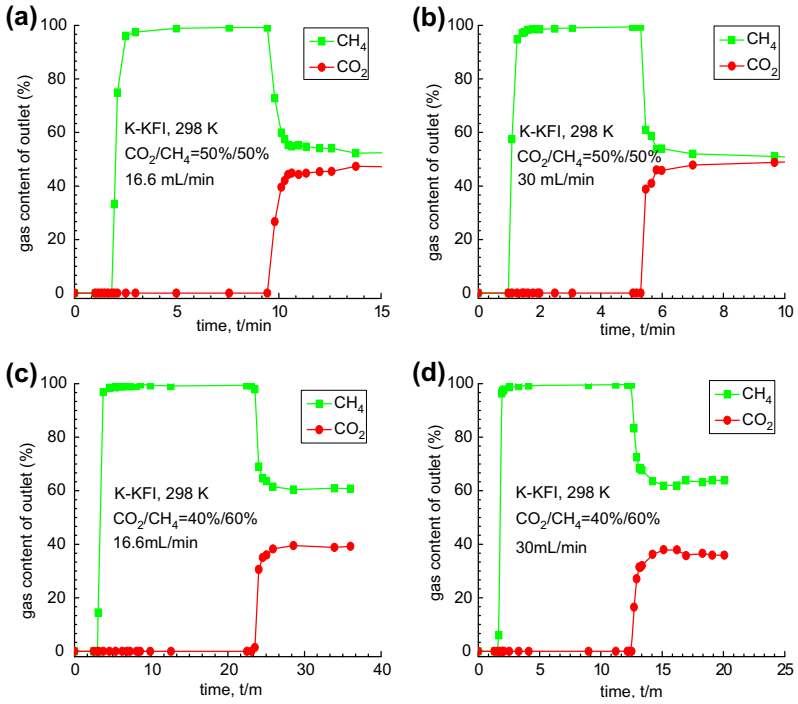

Fig. 5. Breakthrough profiles of CO_2 and CH_4 on K-KFI under atmosphere pressure (CO_2/CH_4 = 50%/50%, 40%/60%).

Table 2
Experiment conditions parameter in literature and our work.

Column	Mass (g)	Density (g/cm^3)	Si/Al	References
Φ4.6 × 100 mm	1.0	0.60	3.67	[22]
Φ9.0 × 150 mm	4.5	0.47	4.59	This work

increased flow rate only reduces the breakthrough time and does not affect the CO_2/CH_4 separation efficiency. The data of Remy et al. (test parameters shown in Table 2) showed that the breakthrough time of CH_4 and CO_2 for K-KFI (Si/Al = 3.67) was 1.2 and 4.2 min, respectively, while for LS K-KFI (Si/Al = 1.67) they were 0.3 and 2.4 min, respectively. Thus, K-KFI with a higher Si/Al content separated these gases more effectively. Although it is not possible to precisely compare our breakthrough experimental data with that of Remy's work because of different operating conditions, our work affords better results; further discussions are provided in the Supplementary material.

The concentration of CO_2 in biogas is generally lower than 50%; thus, we studied the separation of a 40%/60% CO_2/CH_4 mixture in this research. Fig. 5c shows that for this gas mixture the CH_4 breakthrough time increases to 3 min, with CO_2 breakthrough 20 min after; these times are much longer than those for 50%/50% CO_2/CH_4. It can be conclude that increasing the CH_4 concentration also increases the CH_4 adsorption capacity, thus increasing the breakthrough time. Accelerating the mixture-gas flow rate to 30 N mL/min led to CH_4 and CO_2 breakthrough times of 1.58 and 12.5 min, respectively, with the average time shortened by 46%. The breakthrough time decreases linearly with increasing velocity, which also shows the reliability and credibility of the breakthrough experimental data.

For a clearer understanding of the advantages of using K-KFI for CO_2/CH_4 separation, commercial sorbents zeolite 5A and 13X with a 40%/60% CO_2/CH_4 mixture were also investigated. Fig. 6 shows that the breakthrough times of CH_4 and CO_2 in zeolite 5A and 13X are significantly lower than those for K-KFI at both high and low flow rates. Furthermore, the difference between CO_2 and CH_4 breakthrough times was much shorter for the commercial zeolites (see Table 1). As mentioned in the previous publications [30,31], zeolite 13X separated CO_2/CH_4 mixture better than did zeolite 5A. The current study shows that under the same test conditions, the performance of both 13X and 5A are significantly inferior to that obtained with K-KFI (see Table 3); further elaboration is provided in the Supplementary material.

The breakthrough times for CO_2, and CH_4 are compared in Table 3. The capacity of any nanoporous material to capture CO_2 is linearly related to the CO_2 breakthrough time; this is established in earlier works [32–34]. The data presented in Table 3 imply that K-KFI has a significantly higher CO_2 capture potential than commercially available 13X and 5A zeolites.

3.3. Breakthrough simulation

We also conducted simulations of breakthroughs for separation of CO_2/CH_4 mixtures. We found the experimental breakthrough data for CO_2/CH_4 gas mixtures using K-KFI could be simulated extremely well using the methodology described by Krishna and Long [33]. The Supplementary material accompanying this publication provides the details of the breakthrough simulation methodology used here. Experimental validation of the breakthrough simulation methodology used in this work is available in the published literature [34–37]. Comparisons between experimental and simulated data are presented in Fig. 4a and b for 40%/60% CO_2/CH_4 at flow rates of 16.6 and 30 N mL/min, respectively. It is evident that the simulation results for binary mixed-gas separation are consistent with the experimental data (Fig. 7).

Industrial sorbents are sometimes used at pressures much higher than atmospheric pressure. For example, purifying natural gas or biogas by selectively adsorbing CO_2 is often carried out at pressures approaching 2 MPa. To demonstrate the feasibility of producing pure CH_4 from CO_2/CH_4 gas mixtures under high-pressure conditions, we performed breakthrough simulations for 40%/60% mixtures at a total pressure of 2 MPa (see Fig. 8). The breakthrough curves show that pure CH_4 can be recovered in the initial stages of

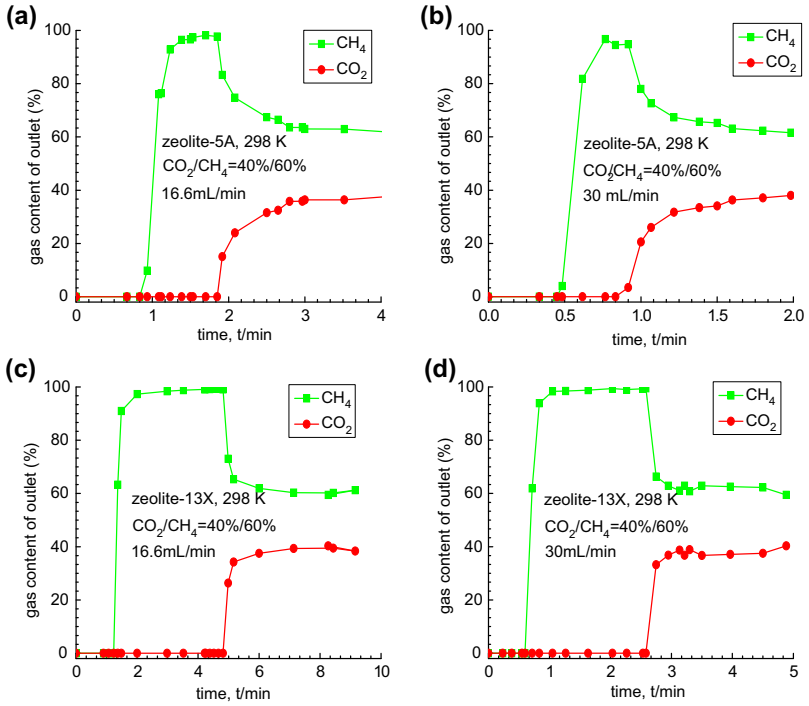

Fig. 6. Breakthrough profiles of CO_2 and CH_4 on zeolite-5A (a, b) and 13X (c, d) under atmosphere pressure (CO_2/CH_4 = 40%/60%).

Table 3
breakthrough times of mixture gases CO_2 and CH_4 for mixture separation with K-KFI, zeolite-5A and 13X at 100 kPa, 298 K.

Samples	CO_2/CH_4	Flow rate (N mL/min)	CH_4 (min)	CO_2 (min)	CO_2–CH_4 (min)	Pressure (MPa)
K-KFI	50%/50%	16.6	1.8	9.4	7.6	0.1
		30.0	1.0	5.3	4.3	0.1
	40%/60%	16.6	3.0	23.0	20.0	0.1
		16.6*	0.7	1.8	1.1	2.0
		30.0	1.6	12.5	11.0	0.1
5A	40/60%	16.6	0.8	1.8	1.0	0.1
		30.0	0.4	0.8	0.4	0.1
13X	40%/60%	16.6	1.2	4.8	3.6	0.1
		30.0	0.6	2.6	2.0	0.1

* Simulation data.

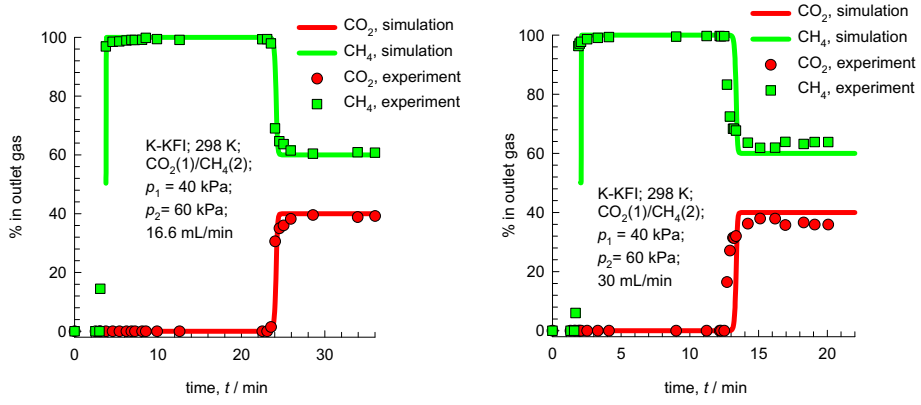

Fig. 7. The simulation of breakthrough profiles of CO_2 and CH_4 on K-KFI under atmosphere pressure (CO_2/CH_4 = 40%/60%).

breakthrough. The breakthrough times of CH_4 and CO_2 on K-KFI were very similar to those for zeolite 5A under atmospheric pressure (Table 3). Therefore, simulate data give a conclusion that K-KFI separates CO_2/CH_4 well even at very high pressures; to the best of our knowledge, this study is the first to report this behavior.

Besides separation in a fixed bed adsorber, K-KFI is also effective for use in membrane permeation devices. The narrow windows separating the cages of K-KFI are expected to be selective to diffusion of CO_2, analogous to permeation across SAPO-34 membrane. For estimation of the membrane permeation selectivities, we use

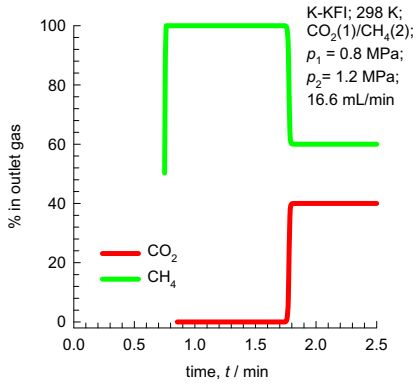

Fig. 8. The simulation of breakthrough profiles of CO_2 and CH_4 on K-KFI under 2 MPa (CO_2/CH_4 = 40%/60%).

the Maxwell–Stefan model discussed in Krishna and van Baten [38] The estimated permeation selectivities are in the range of 150–180, significantly higher than those obtained experimentally for SAPO-34 membranes by Li et al. [39] Further details are provided in the Supplementary material.

4. Conclusion

To study the separation of a CO_2/CH_4 gas mixture, we synthesized and pelletized a K-KFI (Si/Al = 4.59) sorbent. Characterized the sorbent samples using XRD and SEM, and tested their CO_2 and CH_4 adsorption capacities using IGA at a high pressure of 1 MPa. Breakthrough data was collected at ambient temperature and pressure using a mixture-gas separation test system at flow rates of 16.6 and 30 N mL/min. Our breakthrough data showed that the K-KFI sorbent separated the 40%/60% CO_2/CH_4 mixture better than it did the 50%/50% mixture, and separated both mixtures much better than did the commercial sorbents zeolite-5A and 13X under the same conditions. By simulating binary mixture-gas separation, we found the simulated data to be consistent with the experimental data. To demonstrate that pure CH_4 could be separated from CO_2/CH_4 gas mixtures at high pressures, Breakthrough simulations for 40%/60% mixtures at a total pressure of 2 MPa were performed; pure CH_4 was able to be recovered in the initial stages of breakthrough. Therefore, it can be conclude that K-KFI separates CO_2/CH_4 well even at very high pressures; to the best of our knowledge, this study is the first to report this behavior.

Acknowledgement

This work was supported by the National Natural Science Foundation of China (Nos. 21136007, 51302184).

Appendix A. Supplementary data

Supplementary data associated with this article can be found, in the online version, at http://dx.doi.org/10.1016/j.micromeso.2013.09.026.

References

[1] Y.-S. Bae, K.L. Mulfort, H. Frost, P. Ryan, S. Punnathanam, L.J. Broadbelt, J.T. Hupp, R.Q. Snurr, Langmuir 24 (2008) 8592.
[2] S. Cavenati, C.A. Grande, A.E. Rodrigues, Energ. Fuel. 20 (2006) 2648.
[3] A. Yamasaki, J. Chem. Eng. Jpn. 36 (2003) 361.
[4] A. Lohila, T. Laurila, J. Tuovinen, M. Aurela, J. Hatakka, T. Thum, M. Pihlatie, J. Rinne, T. Vesala, Environ. Sci. Technol. 41 (2007) 2717.
[5] S. Cavenati, C.A. Grande, A.E. Rodrigues, Energ. Fuel. 19 (2005) 2545.
[6] E.S. Kikkinides, R.T. Yang, S.H. Cho, Ind. Eng. Chem. Res. 32 (1993) 2714.
[7] J. Yang, Q. Zhao, H. Xu, L. Li, J. Dong, J. Li, J. Chem. Eng. Data 57 (2012) 3701.
[8] P.J.E. Harlick, F.H. Tezel, Sep. Purif. Technol. 33 (2003) 199.
[9] S.M. Kuznicki, V.A. Bell, S. Nair, H.W. Hillhouse, R.M. Jacubinas, C.M. Braunbarth, B.H. Toby, M. Tsapatsis, Nature 412 (2001) 720.
[10] P. Mishra, S. Mekala, F. Dreisbach, B. Mandal, S. Gumma, Sep. Purif. Technol. 94 (2012) 124.
[11] V. Finsy, L. Ma, L. Alaerts, D.E. De Vos, G.V. Baron, J.F.M. Denayer, Micropor. Mesopor. Mat. 120 (2009) 221.
[12] S.T. Zheng, J.T. Bu, Y. Li, T. Wu, F. Zuo, P. Feng, X. Bu, J. Am. Chem. Soc. 132 (2010) 17062.
[13] K. Morishige, J. Phys. Chem. C. 115 (2011) 9713.
[14] X. Liu, J. Li, L. Zhou, D. Huang, Y. Zhou, Chem. Phys. Lett. 415 (2005) 198.
[15] B. Yuan, X. Wu, Y. Chen, J. Huang, H. Luo, S. Deng, Environ. Sci. Technol. 47 (2013) 5474.
[16] H. Yi, F. Li, P. Ning, X. Tang, J. Peng, Y. Li, H. Deng, Chem. Eng. J. 215–216 (2013) 635.
[17] C.A. Grande, R. Blom, A. Möller, J. Möllmer, Chem. Eng. Sci. 89 (2013) 10.
[18] X. Ma, M. Cao, C. Hu, J. Mater. Chem. A. 1 (2013) 913.
[19] Y. Wang, M.D. LeVan, J. Chem. Eng. Data. 55 (2010) 3189.
[20] T. Montanari, G. Busca, Vib. Spectrosc. 46 (2008) 45.
[21] K.S. Walton, M.B. Abney, L.M. Douglas, Micropor. Mesopor. Mat. 91 (2006) 78.
[22] Q. Liu, T. Pham, M.D. Porosoff, R.F. Lobo, ChemSusChem 5 (2012) 2237.
[23] T. Remy, S.A. Peter, L. Van Tendeloo, S. Van der Perre, Y. Lorgouilloux, C.E.A. Kirschhock, G.V. Baron, J.F.M. Denayer, Langmuir 29 (2013) 4998.
[24] M. Miyamoto, Y. Fujioka, K. Yogo, J. Mat. Chem. 22 (2012) 20186.
[25] Y. Li, H. Yi, X. Tang, F. Li, Q. Yuan, Chem. Eng. J. 229 (2013) 50.
[26] I.P. Dzikh, J.M. Lopes, F. Lemos, F. Ramoa Ribeiroa, Appl. Catal. A-Gen. 177 (1999) 245.
[27] Na Young Kang, Bu Sup Song, Chul Wee Lee, Won Choon Choi, Kyung Byung Yoon, Young Ki Park, Micropor. Mesopor. Mat. 118 (2008) 361.
[28] V. Johannes, Zeolite ZK-5. U.S. Patent US4994249, 1991.
[29] S. Schwarz, D.R. Corbin, G.C. Sonnichsen, Micropor. Mesopor. Mat. 22 (1998) 409.
[30] A. Alonso-Vicario, José R. Ochoa-Gómez, S. Gil-Río, O. Gómez-Jiménez-Aberasturi, C.A. Ramírez-López, J. Torrecilla-Soria, A. Domínguez, Micropor. Mesopor. Mat. 134 (2010) 100.
[31] X. Peng, D. Cao, AIChE J. 59 (2013) 2928.
[32] S.C. Xiang, Y. He, Z. Zhang, H. Wu, W. Zhou, R. Krishna, B. Chen, Nat. Commun. 3 (2012) 954.
[33] R. Krishna, J.R. Long, J. Phys. Chem. C. 115 (2011) 12941.
[34] Y. He, R. Krishna, B. Chen, Energy Environ. Sci. 5 (2012) 9107.
[35] E.D. Bloch, W.L. Queen, R. Krishna, J.M. Zadrozny, C.M. Brown, J.R. Long, Science 335 (2012) 1606.
[36] H. Wu, K. Yao, Y. Zhu, B. Li, Z. Shi, R. Krishna, J. Li, J. Phys. Chem. C. 116 (2012) 16609.
[37] Z.R. Herm, B.M. Wiers, J.M. Van Baten, M.R. Hudson, P. Zajdel, C.M. Brown, N. Maschiocchi, R. Krishna, J.R. Long, Science 340 (2013) 960.
[38] R. Krishna, J.M. van Baten, J. Membr. Sci. 430 (2013) 113.
[39] S. Li, J.L. Falconer, R.D. Noble, R. Krishna, J. Phys. Chem. C. 111 (2007) 5075.

Supplementary Material to accompany

Experiments and Simulations on Separating a CO_2/CH_4 Mixture using K-KFI at Low and High Pressures

Jianfeng Yang[a], Rajamani Krishna[b], Junmin Li[a], Jinping Li[a]

a Research Institute of Special Chemicals, Taiyuan University of Technology, Taiyuan 030024, Shanxi, P.R. China

[b]Van 't Hoff Institute for Molecular Sciences, University of Amsterdam, Science Park 904, 1098 XH Amsterdam, The Netherlands

Table of Contents

1. Raw materials used for synthesis of K-KFI

The raw materials used in the synthesis of K-KFI are summarized below.

Chemical Name	Chemical formula	Purity	Producer
alumina	$Al(OH)_3$	99%, Chemical Pure	Aladdin, China
silica sol	SiO_2	40%, Technical Grade	Qingdao Haiyang Chemical Co., Ltd
Strontium nitrate	$Sr(NO_3)_2$	99%, Chemical Pure	Aladdin, China
potassium hydroxide	KOH	96%, Analytical reagent	Tianjin Kemiou Chemical Reagent Co., Ltd.
Deionized water	H_2O		Our lab

We see that all the raw materials are available commercially from suppliers in China. The purity requirements of the raw materials used are also not stringent; so the synthesis does not require expensive raw materials.

2. Optimum conditions for synthesis of K-KFI

The optimum process conditions for synthesis of K-KFI are given below; the specified amounts are molar ratios, taken with respect to Al_2O_3.

Al_2O_3	KOH	SiO_2	$Sr(NO_3)_2$	H_2O	time	temperature
1	3.7	7.1-7.2	0.05-0.15	100-300	5 days	423 K

The synthesis conditions suggest that the production of K-KFI can be carried out on a large scale if required.

3. Effect of Si/Al in raw materials on synthesized K-KFI

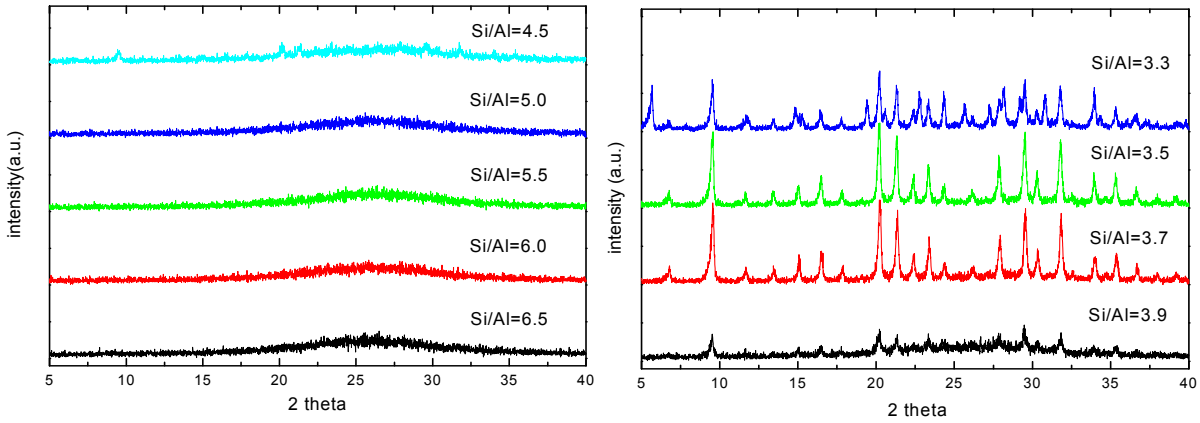

Al_2O_3	KOH	SiO_2	$Sr(NO_3)_2$	H_2O	time	temperature	result
1	3.6	4.0	0.10	130	5 d	423 K	CHA+?
1	3.6	5.0	0.10	130	5 d	423 K	KFI+CHA
1	3.6	6.0	0.10	130	5 d	423 K	KFI+?
1	3.6	7.0	0.10	130	5 d	423 K	KFI
1	3.6	7.1	0.10	130	5 d	423 K	**KFI**
1	3.6	7.2	0.10	130	5 d	423 K	**KFI**
1	3.6	7.3	0.10	130	5 d	423 K	**KFI**
1	3.6	7.4	0.10	130	5 d	423 K	**KFI**
1	3.6	7.5	0.10	130	5 d	423 K	KFI
1	3.6	8.0	0.10	130	5 d	423 K	KFI
1	3.6	9.0	0.10	130	5 d	423 K	NO
1	3.6	10.0	0.10	130	5 d	423 K	NO

4. Effect of Sr/Al ratio on synthesis

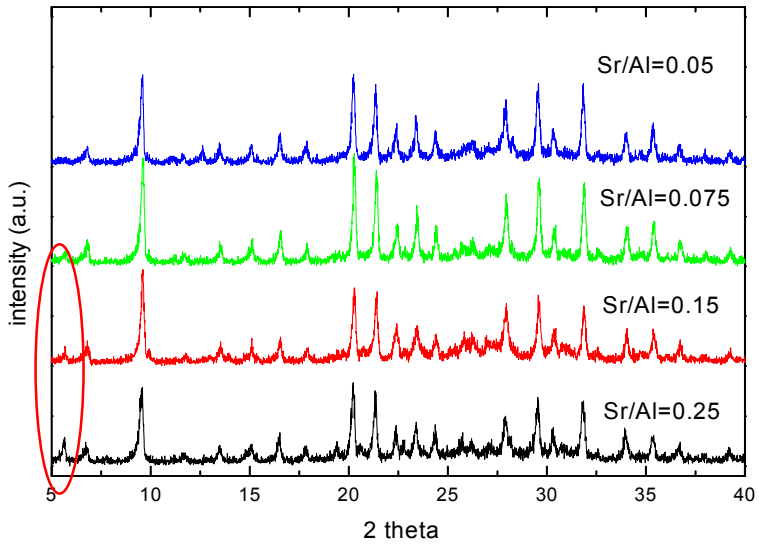

Al_2O_3	KOH	SiO_2	$Sr(NO_3)_2$	H_2O	time	temperature	result
1	3.6	7.2	0.10	130	5 d	423 K	**KFI**
1	3.6	7.2	0.15	130	5 d	423 K	KFI
1	3.6	7.2	0.30	130	5 d	423 K	KFI
1	3.6	7.2	0.50	130	5 d	423 K	KFI

5. Effect of temperature on synthesis

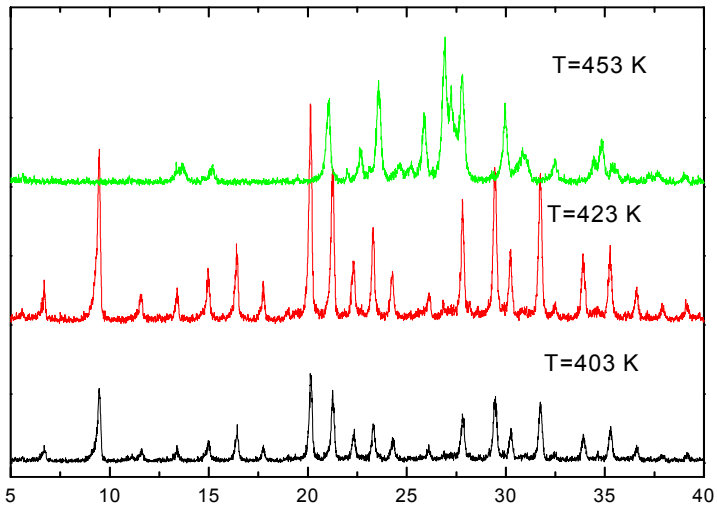

Al_2O_3	KOH	SiO_2	$Sr(NO_3)_2$	H_2O	time	temperature	result
1	3.6	7.2	0.10	130	5 d	403 K	KFI
1	3.6	7.2	0.10	130	5 d	423 K	KFI
1	3.6	7.2	0.10	130	5 d	453 K	unknown

6. Fitting of pure component isotherms for K-KFI

The experimentally measured pure component isotherm data for CO_2, and CH_4 obtained at temperatures at 298 K, up to pressures of 1 MPa are reported by Yang et al.[1] These data were fitted with the Langmuir-Freundlich model

$$q = q_{sat} \frac{bp^{\nu}}{1 + bp^{\nu}} \tag{1}$$

The Langmuir-Freundlich parameters for adsorption of CO_2, and CH_4 in K-KFI are provided in Table 1.

7. Calculations of adsorption selectivity

The selectivity of preferential adsorption of component 1 over component 2 in a mixture containing 1 and 2, perhaps in the presence of other components too, can be formally defined as

$$S_{ads} = \frac{q_1/q_2}{p_1/p_2} \tag{2}$$

In equation (2), q_1 and q_2 are the *absolute* component loadings of the adsorbed phase in the mixture. In all the calculations to be presented below, the calculations of S_{ads} are based on the use of the Ideal Adsorbed Solution Theory (IAST) of Myers and Prausnitz.[2]

Figure 1 presents the IAST calculations of the CO_2/CH_4 selectivities for 50/50 gas mixtures maintained at isothermal conditions at 298 K. The adsorption selectivities for K-KFI are significantly higher than those reported for Cu-TDPAT[3], CuBTC[4], and SAPO-34[5, 6].

8. Packed bed adsorber breakthrough simulation methodology

We performed breakthrough simulations using the methodology described in earlier works.[3, 4, 7-11] Figure 2 shows a schematic of a packed bed adsorber packed with K-KFI.

Assuming plug flow of an *n*-component gas mixture through a fixed bed maintained under isothermal conditions, the partial pressures in the gas phase at any position and instant of time are obtained by solving the following set of partial differential equations for each of the species *i* in the gas mixture.[11-17]

$$\frac{1}{RT}\frac{\partial p_i(t,z)}{\partial t} = -\frac{1}{RT}\frac{\partial\left(v(t,z)p_i(t,z)\right)}{\partial z} - \frac{(1-\varepsilon)}{\varepsilon}\rho\frac{\partial \bar{q}_i(t,z)}{\partial t}; \quad i = 1,2,...n \tag{3}$$

In equation (3), t is the time, z is the distance along the adsorber, ρ is the framework density, ε is the bed voidage, v is the interstitial gas velocity, and $\bar{q}_i(t,z)$ is the *spatially averaged* molar loading within the crystallites of radius r_c, monitored at position z, and at time t.

At any time t, during the transient approach to thermodynamic equilibrium, the spatially averaged molar loading within the crystallites of radius r_c is calculated using

$$\bar{q}_i(t) = \frac{3}{r_c^3}\int_0^{r_c} q_i(t)r^2 dr \tag{4}$$

Summing equation (**4**) over all n species in the mixture allows calculation of the *total average* molar loading of the mixture within the crystallite

$$\bar{q}_t(t,z) = \sum_{i=1}^{n}\bar{q}_i(t,z) \tag{5}$$

The *interstitial* gas velocity is related to the *superficial* gas velocity by

$$v = \frac{u}{\varepsilon} \tag{6}$$

In industrial practice, the most common operation is with to use a step-wise input of mixtures to be separation into an adsorber bed that is initially free of adsorbates, i.e. we have the initial condition

$$t = 0; \quad q_i(0,z) = 0 \tag{7}$$

At time, t = 0, the inlet to the adsorber, z = 0, is subjected to a step input of the n-component gas mixture and this step input is maintained till the end of the adsorption cycle when steady-state conditions are reached.

$$t \geq 0; \quad p_i(0,t) = p_{i0}; \quad u(0,t) = u_0 \tag{8}$$

where u_0 is the superficial gas velocity at the inlet to the adsorber.

The breakthrough characteristics for any component is essentially dictated by the contact time $\frac{L}{v} = \frac{L\varepsilon}{u}$ between the crystallites and the surrounding fluid phase.

If the values of the intra-crystalline diffusivities are large enough to ensure that intra-crystalline gradients are absent and the entire crystallite particle can be considered to be in thermodynamic equilibrium with the surrounding bulk gas phase at that time *t*, and position *z* of the adsorber

$$\bar{q}_i(t,z) = q_i(t,z) \tag{9}$$

The molar loadings at the *outer surface* of the crystallites, i.e. at $r = r_c$, are calculated on the basis of adsorption equilibrium with the bulk gas phase partial pressures p_i at that position *z* and time *t*. The adsorption equilibrium can be calculated on the basis of the IAST.

Equation (9) is commonly invoked for the purposes of screening different nanoporous materials for a given separation task.[3, 7, 9, 10]

Experimental validation of the breakthrough simulation methodology is available in the published literature.[3, 7, 18, 19]

9. Breakthrough simulations vs breakthrough experiments

Yang et al.[20] have presented experimental data or transient breakthrough of 40/60 CO_2/CH_4 mixtures through fixed bed adsorber packed with K-KFI zeolite at flow rates of (a) 16.6 mL/min, and (b) 30 mL/min; see Figures 3a, and 3b. The experimental data are in good agreement with breakthrough simulations that assume thermodynamic equilibrium, i.e. invoking Equation (9).

Figures 4a, and 4b present comparisons of CO_2 breakthroughs for 40/60 CO_2/CH_4 mixtures through fixed beds packed with K-KFI, NaX (=13 X zeolite), and LTA-5A zeolites.

The breakthrough times for CO_2, and CH_4 are compared in Figures 5a, and 5b. The capacity of any nanoporous material to capture CO_2 is linearly related to the CO_2 breakthrough time; this is established

in earlier works.[4, 7, 9] The data presented in Figures 5a, and 5b imply that K-KFI has a significantly higher CO_2 capture potential than commercially available NaX and LTA-5A zeolites.

Remy et al.[21] have reported transient breakthrough experiment data for separation of equimolar CO_2/CH_4 mixtures through fixed bed adsorber packed with K-KFI at 308 K. Their experimental data is re-plotted in Figure 6. We note that their breakthrough times are significantly lower than in the Yang et al.[20] experiments. The main reasons for this are two-fold: (a) they have used a shorter tube, and (b) higher gas velocities within the tube. The contact time between the gas and the K-KFI crystals in their experiments is about a factor 5 lower than in our experiments. Due to the significantly shorter contact times in the experiments of Remy et al,[21] their experiments indicate that intra-crystalline diffusion resistances are of importance. We have established in Figures 3a, and 3b that the Yang et al.[20] experiments can be modeled assuming thermodynamic equilibrium between a crystal and its surrounding gas mixture at any position within the adsorber.

In view of the experimental validation of the breakthrough simulation methodology for K-KFI zeolite, we can proceed with the evaluation of the performance of K-KFI for separation of CO_2/CH_4 gas mixtures under high pressure conditions. The purification of natural gas for selective adsorption of CO_2, is often carried out at pressures approaching 2 MPa. In order to demonstrate the feasibility of producing pure CH_4 from CO_2/CH_4 gas mixtures under high pressure conditions, we carried out breakthrough simulations for 40/60 mixtures at a total pressure of 2 MPa; see Figure 7. We note from the breakthrough curves that it is possible to recover pure CH_4 in the initial stages of the breakthrough.

10. K-KFI membrane permeation

Besides separation in a fixed bed adsorber, K-KFI is also effective for use in membrane permeation devices. The narrow windows separating the cages of K-KFI are expected to be selective to diffusion of CO_2, analogous to permeation across SAPO-34.[5, 6] For estimation of the membrane permeation selectivities, we use the Maxwell-Stefan model discussed in Krishna and van Baten.[22] The Maxwell-Stefan transport coefficients are assumed to have the values $\rho Đ_1/\delta$ = 0.025 kg m^{-2} s^{-1}, and $\rho Đ_2/\delta$ = 0.005 kg m^{-2} s^{-1}. These values yield a diffusion selectivity of 5. Figure 8 presents calculations of the

permeation selectivities for a range of upstream pressures. The estimated permeation selectivities are in the range of 150-180, significantly higher than those obtained experimentally for SAPO-34 membranes by Li et al. [5, 6]

11. Notation

b	Langmuir-Freundlich constant, $Pa^{-\nu}$
L	length of packed bed adsorber, m
p_i	partial pressure of species i in mixture, Pa
p_t	total system pressure, Pa
q_i	component molar loading of species i, mol kg^{-1}
q_t	total molar loading in mixture, mol kg^{-1}
q_{sat}	saturation loading, mol kg^{-1}
R	gas constant, 8.314 J mol^{-1} K^{-1}
S_{ads}	adsorption selectivity, dimensionless
t	time, s
T	absolute temperature, K
u	superficial gas velocity in packed bed, m s^{-1}
z	distance along the adsorber, m

Greek letters

δ	thickness of membrane, m
ε	voidage of packed bed, dimensionless
ν	exponent in Langmuir-Freundlich isotherm, dimensionless
ρ	framework density, kg m^{-3}
τ	time, dimensionless

Table 1. Langmuir-Freundlich parameters for adsorption of CO_2, and CH_4 in K-KFI at 298 K.

	q_{sat} mol kg^{-1}	b_0 $Pa^{-\nu}$	ν dimensionless
CO_2	3.6	2.54×10^{-4}	0.87
CH_4	4.2	1.85×10^{-4}	0.62

12. References

(1) Yang, J.; Zhao, Q.; Xu, H.; Li, L.; Dong, J.; Li, J. Adsorption of CO_2, CH_4, and N_2 on Gas Diameter Grade Ion-Exchange Small Pore Zeolites, *J. Chem. Eng. Data* **2012**, *57*, 3701-3709.

(2) Myers, A. L.; Prausnitz, J. M. Thermodynamics of mixed gas adsorption, *A.I.Ch.E.J.* **1965**, *11*, 121-130.

(3) Wu, H.; Yao, K.; Zhu, Y.; Li, B.; Shi, Z.; Krishna, R.; Li, J. Cu-TDPAT, an *rht*-type Dual-Functional Metal–Organic Framework Offering Significant Potential for Use in H_2 and Natural Gas Purification Processes Operating at High Pressures, *J. Phys. Chem. C* **2012**, *116*, 16609-16618.

(4) Xiang, S. C.; He, Y.; Zhang, Z.; Wu, H.; Zhou, W.; Krishna, R.; Chen, B. Microporous Metal-Organic Framework with Potential for Carbon Dioxide Capture at Ambient Conditions, *Nat. Commun.* **2012**, *3*, 954. http://dx.doi.org/doi:10.1038/ncomms1956.

(5) Li, S.; Falconer, J. L.; Noble, R. D.; Krishna, R. Modeling permeation of CO_2/CH_4, CO_2/N_2, and N_2/CH_4 mixtures across SAPO-34 membrane with the Maxwell-Stefan equations, *Ind. Eng. Chem. Res.* **2007**, *46*, 3904-3911.

(6) Li, S.; Falconer, J. L.; Noble, R. D.; Krishna, R. Interpreting unary, binary and ternary mixture permeation across a SAPO-34 membrane with loading-dependent Maxwell-Stefan diffusivities, *J. Phys. Chem. C* **2007**, *111*, 5075-5082.

(7) He, Y.; Krishna, R.; Chen, B. Metal-Organic Frameworks with Potential for Energy-Efficient Adsorptive Separation of Light Hydrocarbons, *Energy Environ. Sci.* **2012**, *5*, 9107-9120.

(8) He, Y.; Xiang, S.; Zhang, Z.; Xiong, S.; Wu, C.; Zhou, W.; Yildirim, T.; Krishna, R.; Chen, B. A microporous metal-organic framework assembled from an aromatic tetracarboxylate for H_2 purification, *J. Mater. Chem. A* **2013**, *1*, 2543-2551.

(9) Krishna, R.; Long, J. R. Screening metal-organic frameworks by analysis of transient breakthrough of gas mixtures in a fixed bed adsorber, *J. Phys. Chem. C* **2011**, *115*, 12941-12950.

(10) Krishna, R.; van Baten, J. M. A comparison of the CO_2 capture characteristics of zeolites and metal-organic frameworks, *Sep. Purif. Technol.* **2012**, *87*, 120-126.

(11) Krishna, R.; Baur, R. Modelling issues in zeolite based separation processes, *Sep. Purif. Technol.* **2003**, *33*, 213-254.

(12) Ruthven, D. M. Principles of Adsorption and Adsorption Processes; John Wiley: New York, 1984.

(13) Ruthven, D. M.; Farooq, S.; Knaebel, K. S. Pressure swing adsorption; VCH Publishers: New York, 1994.

(14) Yang, R. T. Gas separation by adsorption processes; Butterworth: Boston, 1987.

(15) Do, D. D. Adsorption analysis: Equilibria and kinetics; Imperial College Press: London, 1998.

(16) van den Broeke, L. J. P.; Krishna, R. Experimental Verification of the Maxwell-Stefan Theory for Micropore Diffusion, *Chem. Eng. Sci.* **1995**, *50*, 2507-2522.

(17) Walton, K. S.; LeVan, M. D. Consistency of Energy and Material Balances for Bidisperse Particles in Fixed-Bed Adsorption and Related Applications, *Ind. Eng. Chem. Res.* **2003**, *42*, 6938-6948.

(18) Bloch, E. D.; Queen, W. L.; Krishna, R.; Zadrozny, J. M.; Brown, C. M.; Long, J. R. Hydrocarbon Separations in a Metal-Organic Framework with Open Iron(II) Coordination Sites, *Science* **2012**, *335*, 1606-1610.

(19) Herm, Z. R.; Wiers, B. M.; Van Baten, J. M.; Hudson, M. R.; Zajdel, P.; Brown, C. M.; Maschiocchi, N.; Krishna, R.; Long, J. R. Separation of Hexane Isomers in a Metal-Organic Framework with Triangular Channels *Science* **2013**, *340*, 960-964.

(20) Yang, J.; Li, J.; Li, J. Experiments and Simulations on Separating a CO_2/CH_4 Mixture using K-KFI at Low and High Pressures, *Microporous Mesoporous Mater.* **2013**, *Submitted for publication*,

(21) Remy, T.; Peter, S. A.; Van Tendeloo, V.; Van der Perre, S.; Lorgouilloux, Y.; Kirschhock, C. E. A.; Baron, G. V.; Denayer, J. F. M. Adsorption and Separation of CO_2 on KFI Zeolites: Effect of Cation Type and Si/Al Ratio on Equilibrium and Kinetic Properties, *Langmuir* **2013**, *29*, 4998-5012.

(22) Krishna, R.; van Baten, J. M. Investigating the Influence of Diffusional Coupling on Mixture Permeation across Porous Membranes *J. Membr. Sci.* **2013**, *430*, 113-128.

13. Captions for Figures

Figure 1. Calculations using Ideal Adsorbed Solution Theory (IAST) of Myers and Prausnitz[2] for 50/50 CO_2/CH_4 selectivities for equimolar gas mixtures maintained at isothermal conditions at 298 K. Also shown are the adsorption selectivities for Cu-TDPAT[3], CuBTC[4], and SAPO-34[5, 6].

Figure 2. Schematic of a packed bed adsorber.

Figure 3. (a, b) Experimental data of Yang et al.[20] for transient breakthrough of 40/60 CO_2/CH_4 mixtures through fixed bed adsorber packed with K-KFI zeolite. The experimental data (symbols) of Yang et al.[20] at flow rates of (a) 16.6 mL/min, and (b) 30 mL/min are compared with breakthrough simulations that assume thermodynamic equilibrium, i.e. invoking Equation (9). The parameter values for bed length L, voidage of bed, interstitial gas velocity, v are taken from the experimental set-up and operating conditions.

Figure 4. (a, b) Experimental data of Yang et al.[20] comparing the CO_2 breakthroughs for 40/60 CO_2/CH_4 mixtures through fixed beds packed with K-KFI, NaX (=13 X zeolite), and LTA-5A zeolites at flow rates of (a) 16.6 mL/min, and (b) 30 mL/min.

Figure 5. (a, b) Experimental data, presented in Table 3 of Yang et al.,[20] comparing the and CH_4 and CO_2 breakthroughs for 40/60 CO_2/CH_4 mixtures through fixed beds packed with K-KFI, NaX (=13 X zeolite), and LTA-5A zeolites at flow rates of (a) 16.6 mL/min, and (b) 30 mL/min.

Figure 6. Transient breakthrough experiments of Remy et al.[21] for equimolar CO_2/CH_4 mixtures through fixed bed adsorber packed with K-KFI at 308 K.

Figure 7. Simulated breakthrough 40/60 CO_2/CH_4 mixture using K-KFI for inlet gas flow rate of 16.6 mL/min and total pressure of 2 MPa.

Figure 8. Calculation of the permeation selectivities for separation of 50/50 CO_2/CH_4 mixture using K-KFI membrane. The calculations are for a range of upstream pressures, using the simplified analytic model discussed in Krishna and van Baten.[22] The estimations are based on the values of $\rho Đ_1/\delta = 0.025$ kg m^{-2} s^{-1}, and $\rho Đ_2/\delta = 0.005$ kg m^{-2} s^{-1}.

Figure 1

Adsorption selectivity from IAST

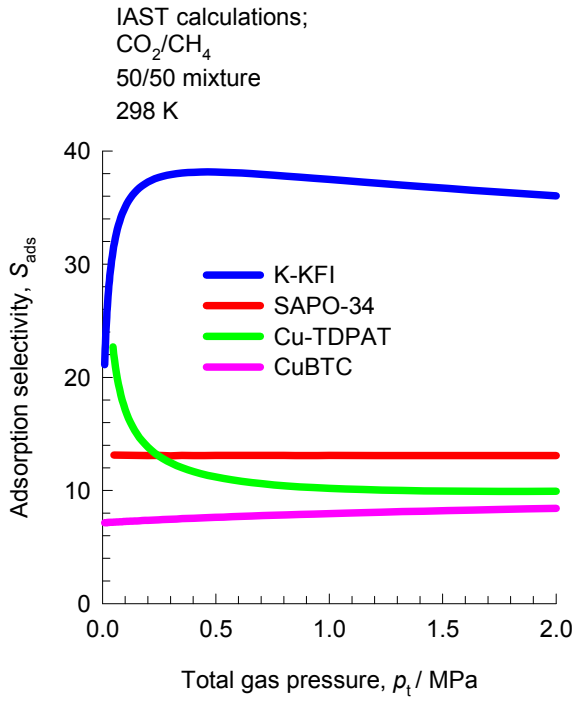

Figure 2

Fixed bed adsorber

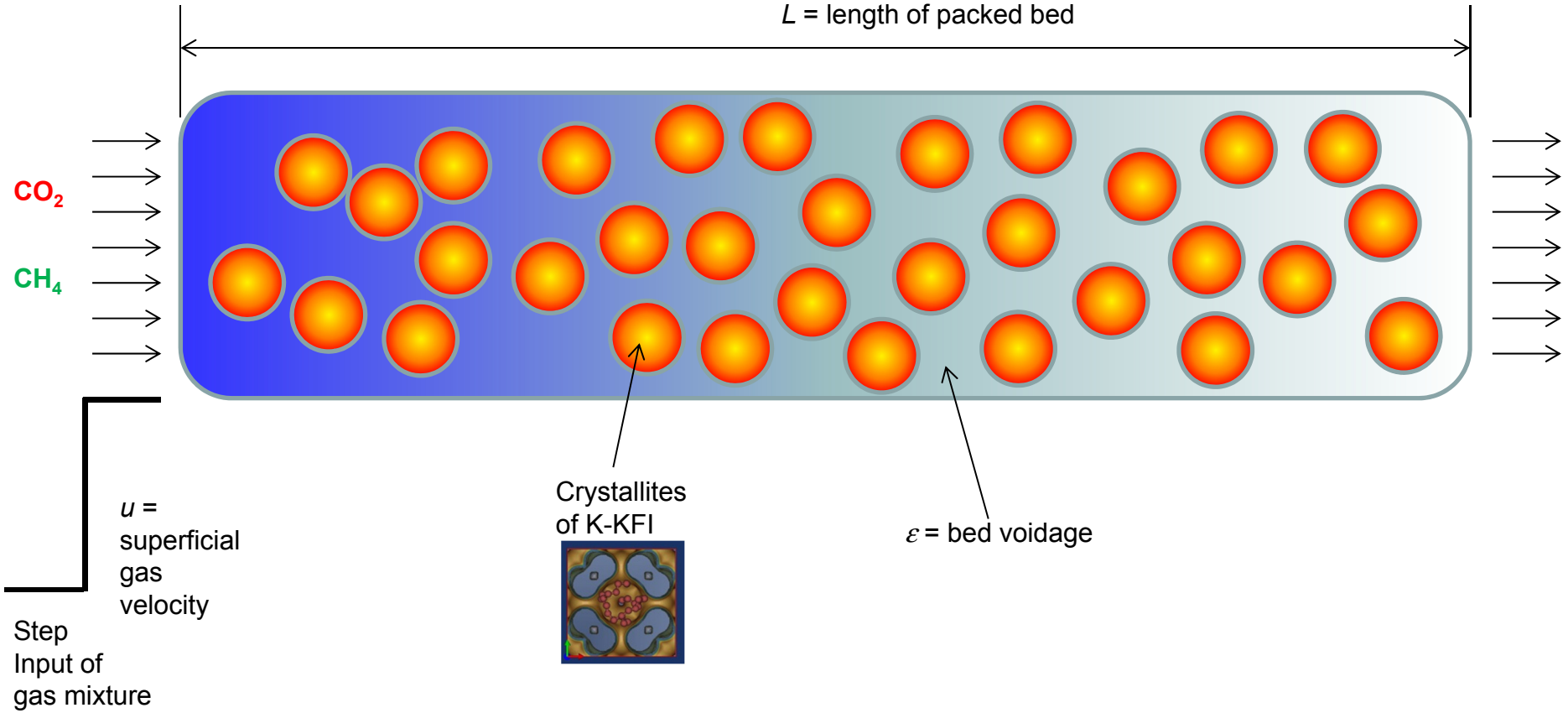

Experiment vs Simulation CO_2/CH_4 separation with K-KFI

Figure 3

KFI

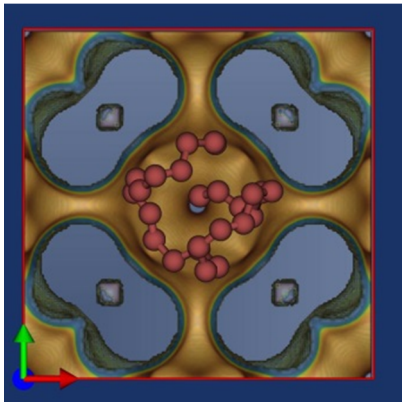

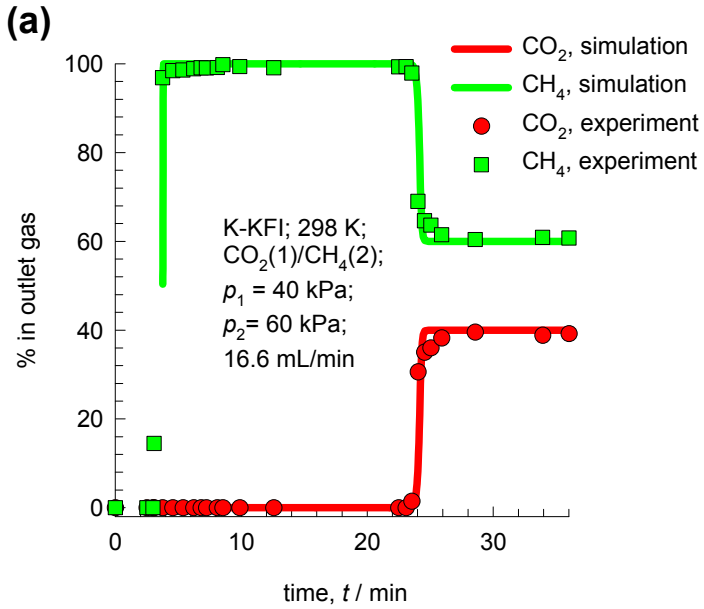

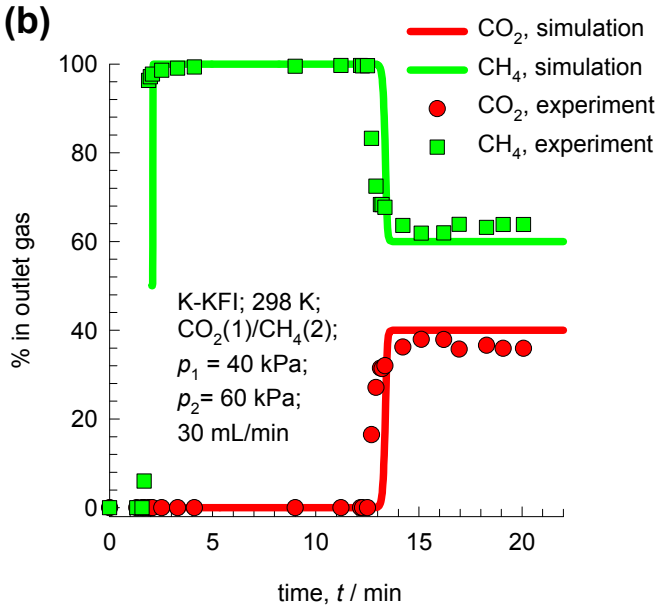

Figure 4

CO_2/CH_4 separation with K-KFI, 13X and LTA-5A

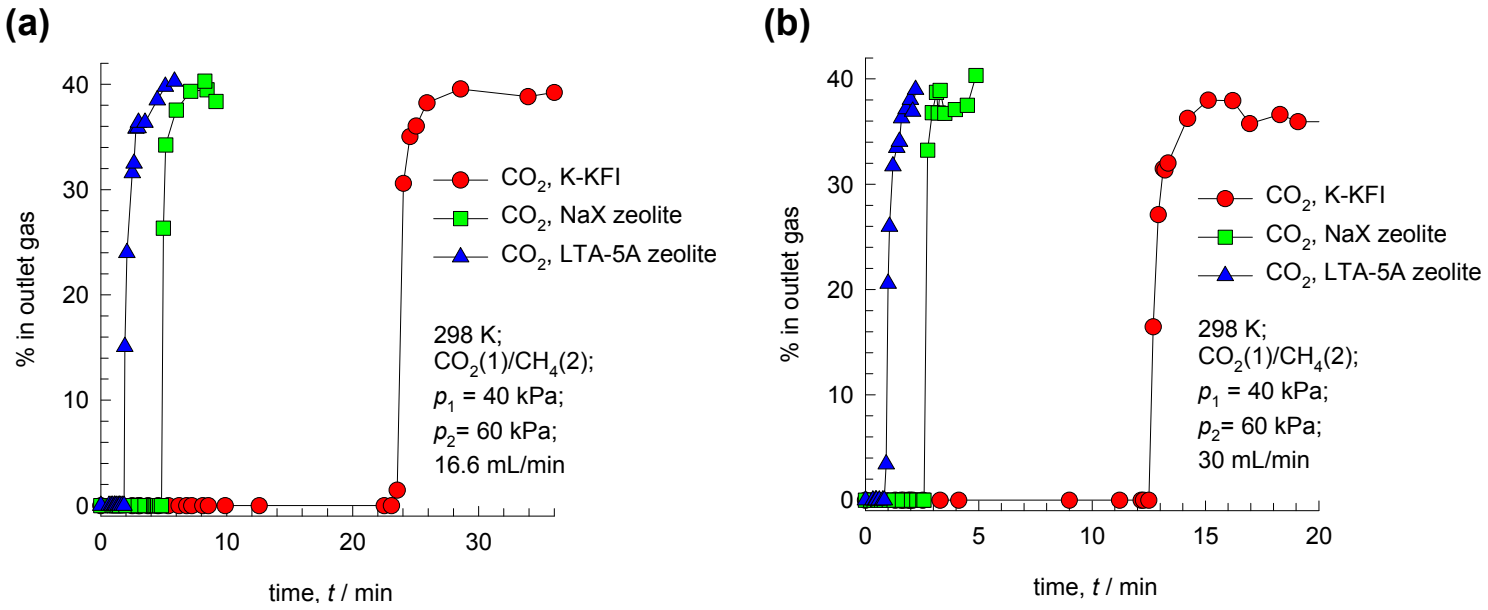

Figure 5

CO_2/CH_4 separation: comparison of breakthrough times

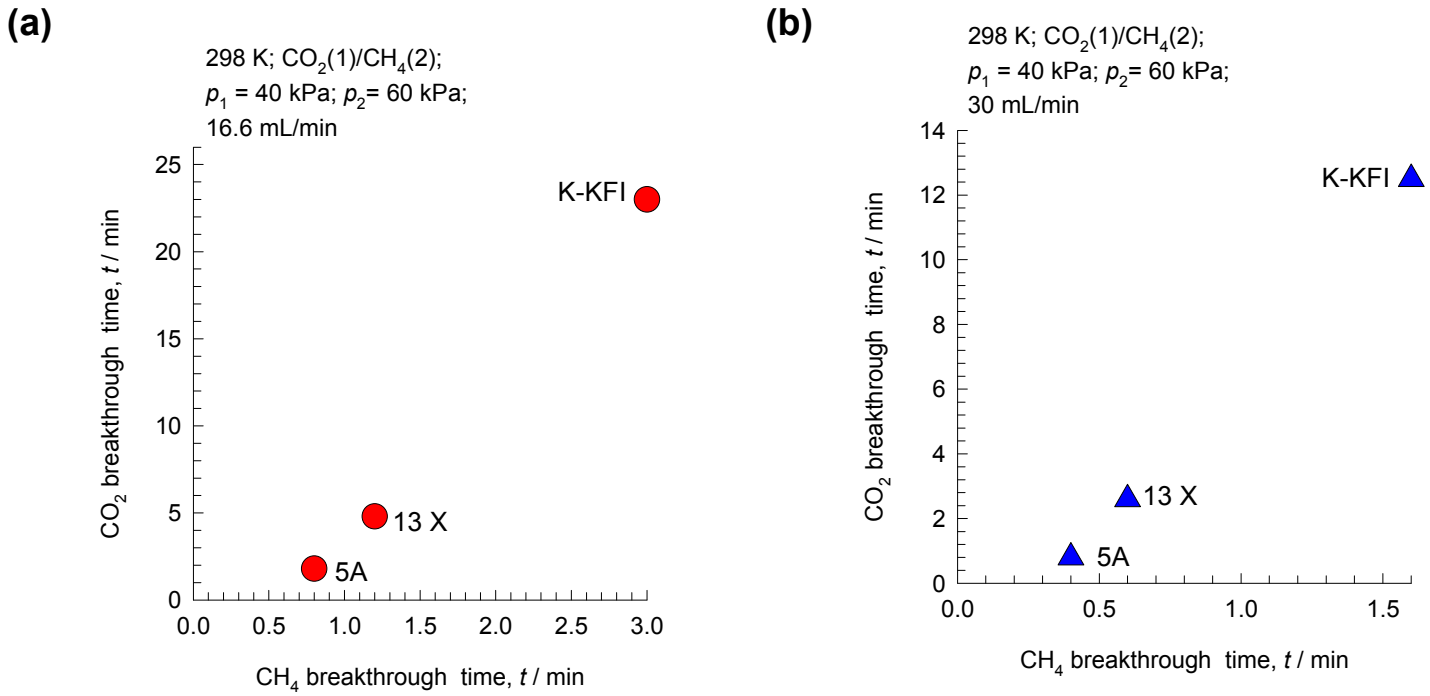

Figure 6

CO_2/CH_4 separation: Expt data of Remy

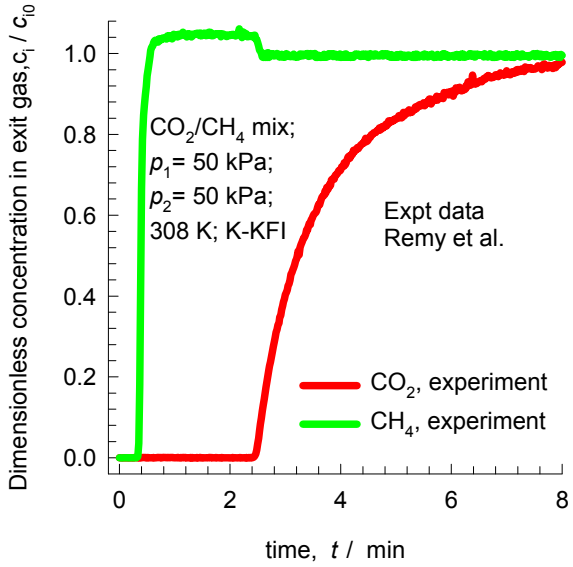

Figure 7

CO_2/CH_4 breakthrough in fixed bed adsorber at 2 MPa

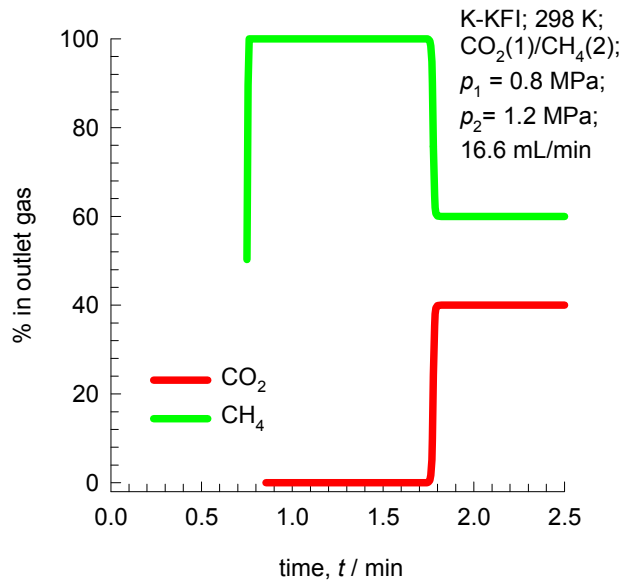

Figure 8

CO_2/CH_4 permeation across membrane